![TU Delft logo]

Delft University of Technology

GMPP Estimator as a Global Solution for MPPT Algorithms Under Partial Shading Conditions

Sangrody, R.; Taheri, S.; Cretu, A. -M.; Pouresmaeil, E.; Vahedi, H.

Important note
To cite this publication, please use the final published version (if applicable).
Please check the document version above.

GMPP Estimator as a Global Solution for MPPT Algorithms Under Partial Shading Conditions

REZA SANGRODY[1], SHAMSODIN TAHERI [1] (Senior Member, IEEE),
ANA-MARIA CRETU [1] (Senior Member, IEEE), EDRIS POURESMAEIL [2] (Senior Member, IEEE),
AND HANI VAHEDI [3] (Senior Member, IEEE)

[1]Department of Computer Science and Engineering, University of Quebec in Outaouais, Gatineau, QC J8X 3X7, Canada
[2]Department of Electrical Engineering and Automation, Aalto University, 02150 Espoo, Finland
[3]Department of Electrical Engineering, Mathematics and Computer Science, Delft University of Technology, 2628 CP Delft, The Netherlands

CORRESPONDING AUTHOR: SHAMSODIN TAHERI (e-mail: shamsodin.taheri@uqo.ca).

ABSTRACT The power versus voltage curve of a photovoltaic (PV) panel exhibits several maximum power points (MPPs) in a partial shading (PS) condition. Thus, it remains an optimization challenge to ensure that PV systems operate at their global MPP (GMPP). Scanning the output characteristics of the PV panels seems a general solution for this issue. However, applying a short circuit to the terminal of PV panels where there exists an electrolytic capacitor, has a detrimental effect on the lifetime of the system. To this end, in this article, a GMPP estimator is proposed as a global solution for conventional maximum power point tracking (MPPT) algorithms under PS conditions. The proposed technique improves existing simple MPPT algorithms with original approaches as follows: first, an accurate microscopic analysis of a PV characteristic in PS conditions is considered, second, an original definition of the dominant cells and modules in a PV panel is proposed that allows to reduce the PS patterns to a finite number, and third, the search area for the MPPT operation is reduced to find the accurate GMPP by proposing two voltage boundaries. The lower boundary corresponds to the GMPP under uniform shading condition that can be determined using a closed form formula, while the upper one refers to the GMPP of a dominant cell in a PV module that can be determined using an artificial intelligence technique. This can also help set the initial duty cycle in a convex area around the GMPP. The functionality of the proposed GMPP estimator is experimentally validated.

INDEX TERMS Dominant cell, dominant module, global maximum power point (MPP) (GMPP) estimation, hill climbing algorithm, partial shading (PS) pattern, steady-state oscillation.

I. INTRODUCTION

Photovoltaic (PV) energy is a promising solution in addressing climate change and long-term energy security. However, the energy efficiency of PV systems can be negatively affected when individual modules of a PV array receive unequal amounts of solar irradiance, known as a partial shading (PS) phenomenon. This condition changes the number of maximum power points (MPPs) and varies the voltage value of global MPP (GMPP) significantly [1], [2], [3].

The PS phenomenon has been interpreted in two different ways, i.e., macroscopic and microscopic analyses.

Macroscopic analysis refers to a different, uniform irradiation distribution on PV panels of an array. Thus, the PS condition happens to an array rather than a panel resulting in multiple peaks in the equivalent current–voltage (I–V) curve of the array [4], [5], [6], [7], [8]. This analysis is suitable for string inverter applications. The microscopic analysis refers to a PS as an uneven irradiation pattern on a PV panel in which one or a number of cells have different shading conditions due to some obstacles, such as peripheral objects, snow, bird droppings, and dust. In comparison with the macroscopic analysis, this analysis shows an accurate and real behavior

of an electrical characteristic of a PV system under PS conditions. Thus, this analysis is considered in the present contribution to ensure that PV systems operate at their GMPP rather than at local ones under PS conditions.

Existing inverters on the market are commonly equipped with traditional maximum power point tracking (MPPT) controllers such as the Hill climbing (HC) [9] and the perturb and observe (P&O) techniques with a similar fundamental approach to achieve the MPP [10]. Although these MPPT techniques have simple control mechanisms and are easy to be implemented, they can only find the single MPP under uniform irradiation patterns. These methods fail to track the GMPP under PS conditions where the electrical characteristics of the PV panel bear multiple peaks, not to mention a slow convergence and power fluctuations in the steady state. Two solutions are offered to address the MPPT problems in this condition. In the first solution, the MPPT algorithm basically is implemented by a traditional method and a heuristic method accompanies it to improve its performance. For example, the P&O technique was improved by integrating with grey wolf optimization [11], combining with particle swarm optimization [12], or modifying its algorithm [13], [14]. In the second category, this algorithm is completely based on the heuristic optimization techniques such as team game optimization [15], firefly algorithm [16], grey wolf optimization [17], particle swarm optimization [18], whale optimization [19], simulated annealing [20], artificial bee colony [21], ant colony optimization [22], cuckoo search [23], and voltage and current perturbation [24]. Each solution has been able to address a particular issue of those including getting stuck in a local maximum power point (LMPP), slow convergence time and power fluctuations in the steady state.

Scanning the I–V curve directly by changing the current or voltage of a PV panel from zero to its short-circuit current or open-circuit voltage value was used in [25], [26], [27], [28], [29]. This method has several advantages such as estimating the GMPP value very fast, avoiding getting stuck in the LMPP, detecting the occurrence of the PS conditions and all required information about the situation of PV panels. However, the electrolytic capacitor at the PV panel terminal can be degraded or failed due to its regular charging and discharging during the I–V curve scanning. Moreover, because of voltage transient response of the electrolytic capacitor in parallel with the PV panel, a high current during the scanning procedure is inevitable. Another way to estimate the GMPP is based on a prepared dataset using a PV cell model. Then, an artificial intelligence (AI) model is built using the dataset to estimate the GMPP [30], [31], [32], [33]. However, in these research works, the irradiation value on each PV panel is uniform and PS condition is supposed as a different irradiation value on one or some PV panels in an array of PV panels (macroscopic analysis). While, in reality, the shading pattern on a PV panel can be uneven (microscopic analysis). This causes an increase in the voltage value at the GMPP in comparison with the even shading condition, therefore, the accurate GMPP cannot be calculated. The problem regarding the microscopic analysis

is that there are infinite number of shading patterns on a PV panel and each pattern creates a unique I–V curve. On the other hand, having information about the shading pattern is not straightforward. Digital camera and image processing can be used to detect the PS pattern [34], [35], [36], [37], [38] and consequently the dominant cells of a PV panel. But this method increases the complexity and price of the system and its implementation is not feasible in every situation.

To overcome the above mentioned issues, and due to lack of a sophisticated method for harvesting the maximum energy from a PV system in a reliable and efficient way in PS conditions, a novel GMPP estimator is proposed, which helps achieve a high penetration of solar systems. To this end, as a first contribution, a microscopic analysis of the PS condition is taken into account for modeling. Then, as a second contribution, for an accurate and effective analysis of PS conditions, the concept of a dominant cell in a module of a PV panel is proposed that can reduce the number of infinite PS patterns to a set of finite ones. Finally, as a third contribution, two voltage boundaries, i.e., the lower voltage and upper voltage are proposed in PS conditions in which the voltage at the GMPP occurs. The lower voltage corresponds to the GMPP under uniform shading condition that can be determined using a closed-form formula. The upper voltage refers to the GMPP of a dominant cell in a PV module. Since this upper voltage is affected by temperature, irradiation, and PS depth in a nondeterministic way, an AI technique is used for its estimation. In addition, the AI technique can be used as an initial condition estimator for the MPPT algorithm. The proposed technique has capability to improve any existing MPPT techniques suffering from the complexity, accuracy in tracking the GMPP, cost, and speed. The effectiveness of the proposed technique in tracking the GMPP with rapid convergence and small fluctuations is validated numerically and experimentally through its application to a conventional HC MPPT algorithm.

The rest of this article is organized as follows. In Section II, the scanning method and the effects of microscopic analysis are discussed. Then, the concept of dominant cell and module in a PV panel are introduced and the GMPP boundaries and using AI to estimate these boundaries in PS conditions are explained in Sections III and IV. The experimental results of using the proposed method in an MPPT algorithm are presented in Section V. Finally, Section VI concludes this article.

II. SCANNING METHOD EFFECTS AND MICROSCOPIC ANALYSIS

The boost converter, connected to the terminal of the PV panels to implement the MPPT algorithm and to increase the level of voltage, is able to perform the scanning method. Fig. 1 shows the implementation of this method and its operation on the I–V curve. First, the system is operating at point OP, then the MOSFET of the converter turns ON to create a short circuit at the terminal of the PV panel. When the voltage of the PV panel reaches zero, the MOSFET turns OFF and measuring the PV voltage and current is started to sweep the I–V curve.
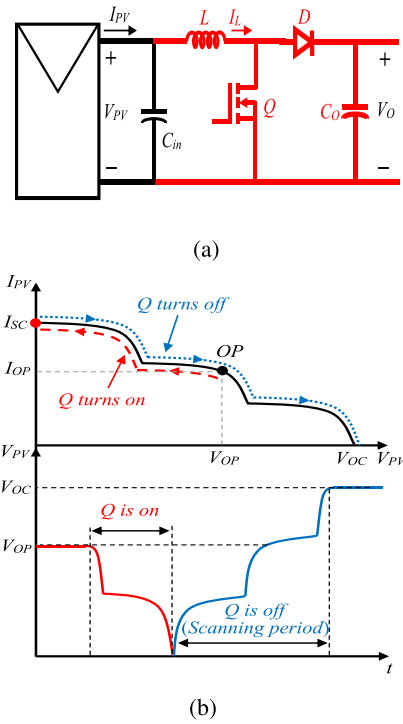
(a)

(b)

FIGURE 1. Boost power optimizer scanning method. (a) Boost power optimizer. (b) Scanning trajectories for the boost converter.

FIGURE 2. Short-circuit current flowed toward the MOSFET.

(a)

(b)
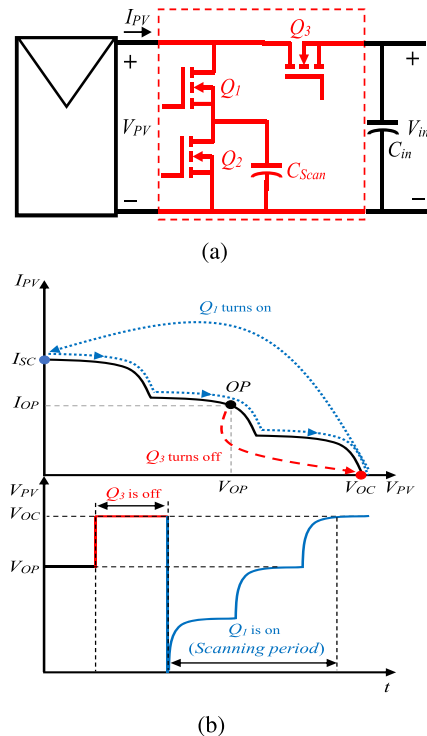
FIGURE 3. Specialized circuit for scanning the *I–V* curve. (a) Specialized circuit. (b) Scanning trajectories.

Supposing the shading condition on the PV panel is even, therefore, the PV panel is almost a current source when a short circuit is applied to its terminals and its current is almost equal to I_{OP} at the left-hand side of point OP. In this condition, (1) shows the current of the MOSFET (i_{Mos}) when it turns ON to create a short-circuit supposing negligible resistance of the inductor (L), capacitor (C), and MOSFET

$$i_{\mathrm{Mos}}(t) = I_{\mathrm{OP}} + i_{\mathrm{Res}}(t)$$

$$i_{\mathrm{Res}}(t) = I_{\mathrm{OP}} \cos\left(\omega_r t\right) - V_{\mathrm{OP}}\sqrt{\frac{C}{L}} \sin\left(\omega_r t\right)$$

$$= I_{\max} \sin\left(\omega_r t - \varphi\right)$$

$$\omega_r = \frac{1}{\sqrt{LC}} \ , \ I_{\max} = \sqrt{I_{\mathrm{OP}}^2 + \frac{C}{L}V_{\mathrm{OP}}^2} \tag{1}$$

where ω_r, I_{OP}, V_{OP}, C, L, and $I_{\max}$ are the resonance frequency, operating current, operating voltage, terminal capacitor value, inductor value, and the maximum current value, respectively. Fig. 2 exhibits a typical current, which shows applying a short-circuit causes a high amount of current, therefore, it damages the electrolytic capacitor, and as a result, the interval between two consecutive scans should be long enough to avoid increasing the temperature of this capacitor. In addition, the nominal current of the MOSFET should be higher compared to the current of the MOSFET in a nonscanning power optimizer. Fig. 3 is another implementation to solve this problem. As seen, Q_3 is used to disconnect the
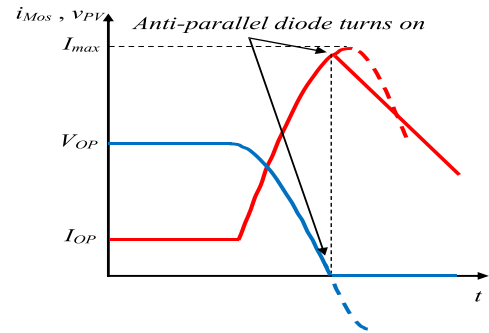
terminal capacitor from the PV panel then the scanning procedure starts by turning ON Q_1 and charging C_{Scan}. Also, Q_2 is used to discharge C_{Scan} and to reset the circuit for the next scan. The terminal capacitor is not affected by the scanning operation; therefore, its lifetime in this scanning method is the same as in a PV system without any scanning circuit. However, C_{Scan} that is an electrolytic capacitor sinks this current and is affected by its detrimental effects.

The information acquired by the scanning method seems suitable but as explained, its detrimental effect on the lifetime of the system is inevitable; therefore, it is not a favorable method in a real application. On the other hand, all this information such as the short-circuit current of all PV panels, the open-circuit voltage, and the number of PV panels in
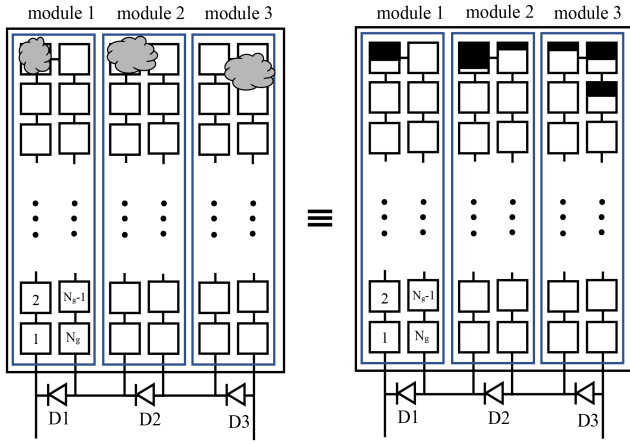
FIGURE 4. Typical PV panel in PS condition.

the PS condition is not necessary for a lot of applications such as the MPPT algorithm. In these applications, having knowledge about the voltage value at the GMPP is enough. Consequently, another method should be designed to have a real-time feedback, especially in PS conditions similar to the scanning method without any detrimental effect on the system. From this perspective, preparing a dataset and applying an AI technique are promising. But the problem is that there are an infinite number of PS patterns for a PV panel, each one with its own *I–V* curve. Therefore, a method should be devised to limit the number of PS patterns on a PV panel. On the other hand, evaluating and quantifying a PS pattern as the input of the AI tool should be done by the terminal boost converter to avoid extra cost and complexity caused by a separate data preparation circuit.

III. PS MODELING USING DOMINANT CELL AND MODULE IN A PV PANEL

As previously mentioned, there are an infinite number of PS patterns for a PV panel, each one with its own *I–V* curve. Therefore, there is one GMPP for each pattern and it seems impossible to estimate the GMPP for all these patterns. But it can be shown that the number of PS patterns can be decreased by knowing its mechanism and defining some simple terms as follows.

Each PV panel consists of several modules of PV cells, where a module of cells consists of a number of series cells that are in parallel with a diode. Depending on the pattern of PS, a number of cells in each module may be in a shading condition. For example, Fig. 4 shows a typical PV panel covered by snow with three modules of cells, each module has N_g cells, which one cell in module 1, two cells in module 2 and three cells in module 3 are under PS conditions. The shaded cells are shown by the black area and a bigger black area means bigger shading area. Two terms, namely dominant cell and dominant module can be defined to evaluate the effect of the PS condition on the *I–V* curve of a PV panel and consequently on the MPP position. The *I–V* curve of each cell can be
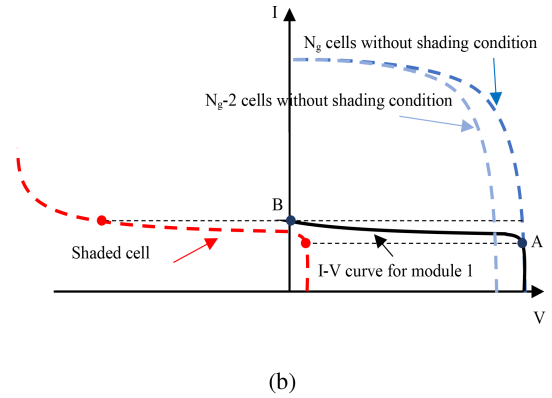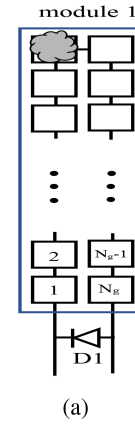

FIGURE 5. *I–V* curve of module 1.

achieved by the well-known one diode model as shown in the following equation:

$$I_C = K_{sh}I_{ph} - I_o \left(e^{\frac{q(V_C+R_SI_C)}{aK_tT}} - 1 \right) - \frac{(V_C+R_SI_C)}{R_P}$$
$$\times \left(1 + K_d \left(1 - \frac{(V_C+R_SI_C)}{V} \right)^{-n_d} \right) \qquad (2)$$

where I_{ph}, I_o, R_S, R_P, a, q, K_t, T, K_d, n_d, and V_{br} are photo-generated current, inverse saturation current, series and parallel resistance, diode ideality factor, electron charge, Boltzmann constant, temperature in Kelvin, fraction of current involved in avalanche breakdown, avalanche breakdown exponent, and breakdown voltage, respectively. In PS conditions, the photo-generated current of shaded cell has to be multiplied by a coefficient depending on the depth and extension of shading area on the shaded cell (K_{sh}) [34]. Also, the reverse part of (2) should be regarded because the shaded cell works in the reverse area of its *I–V* curve.

Fig. 5 shows the *I–V* curves related to the module 1 in Fig. 4 including one shaded cell and $N_g - 1$ unshaded cells. As can be seen, before the point A, the equivalent *I–V* curve is almost the same as in the nonshading condition. As soon as the current value tends to be increased, the *I–V* curve is affected by the shaded cell until it reaches the point B. After this point, the terminal voltage of this module tends to be
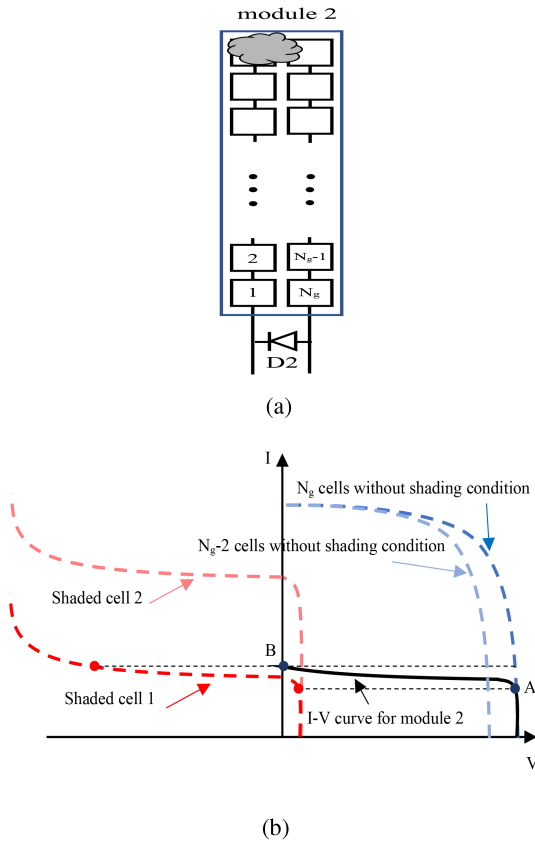
(a)

FIGURE 6. *I–V* curve of module 2.

FIGURE 7. *I–V* curve boundary of a module.

(b)

FIGURE 8. *I–V* curve of PV panel.

negative, therefore, its parallel diode becomes forward biased and the terminal voltage stays at a zero value. Fig. 6 illustrates the same process for module 2 of Fig. 4, in which two cells are in PS conditions. Dashed red lines show the *I–V* curve of shaded cells and the pale blue line depicts this curve for the remaining cells in nonshading conditions. Before point A, the *I–V* curve of this module is almost the same as the dark blue dashed line, which is associated with the condition when all cells are in a nonshading situation. But, after point A, the curve is affected by that of cell 1, which has the deepest shading condition. It means that K_{sh} of this cell in (2) is less than the other shaded cell. In other words, in each module of PV cells which is in PS condition, the *I–V* curve of the module is dominantly affected by the cell that has the lowest K_{sh}. This cell is called a dominant cell in this article. In fact, two modules have almost the same *I–V* curve if their dominant cells have the same conditions, and other cells in these modules have a small effect on their *I–V* curve. This small effect goes back to the open-circuit voltage of a module, which is the sum of open-circuit voltage of its cells. The open-circuit voltage changes slightly with different irradiation values. Also, the short-circuit current varies in a small range by increasing the number of shaded cells consequently, the *I–V* curves appear in the form of Fig. 7 associated to one cell (dominant cell) in a shading condition and to other remaining cells with the same irradiation equal to the dominant cell (even irradiation
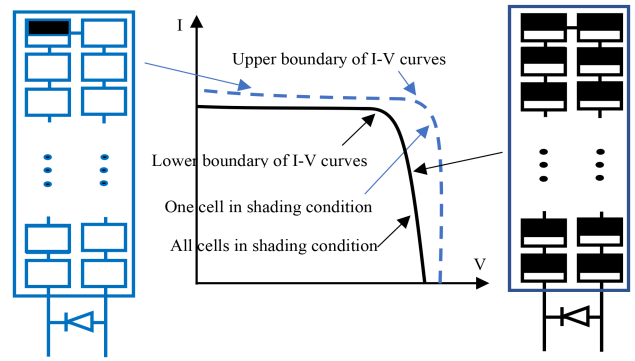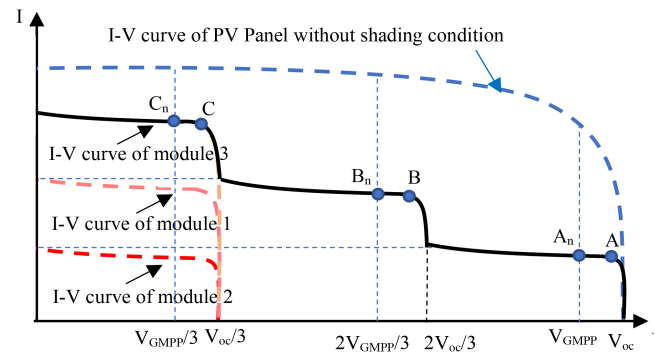
curve). Therefore, knowing the GMPP of these boundaries can provide the required information to identify the GMPP. The same procedure can be considered for modules that generate the *I–V* curve of a panel. Fig. 8 shows typical *I–V* curves of three modules highlighted in Fig. 4 as well as the equivalent *I–V* curve of the PV panel. By increasing the current from zero to the short-circuit current level, the diode of module 2 becomes forward biased before those of module 1 and finally module 3. In fact, the higher generated power usually occurs in a higher voltage in the *I–V* curve of a PV panel. Therefore, module 2 can be defined as the dominant module of this panel because it determines the *I–V* curve of the PV panel in higher voltage ranges.

IV. GMPP BOUNDARIES ESTIMATION IN PS CONDITIONS
As shown in Fig. 7, the electrical characteristic of a PV panel under PS conditions happens in a zone between the lower and upper boundaries. The lower and upper boundaries are related to the electrical characteristics of a PV panel under even and uneven irradiation, respectively. Fig. 9 highlights the voltage value at the GMPP of a PV panel under even (V_{G_E}) and uneven (V_{G_U}) irradiation. The solid curves are associated to the condition when all cells have the same shading depth (even shading) and the dashed line represents the situation when just one cell has this value of shading depth. V_{G_E} can be calculated analytically and in a closed-form equation,
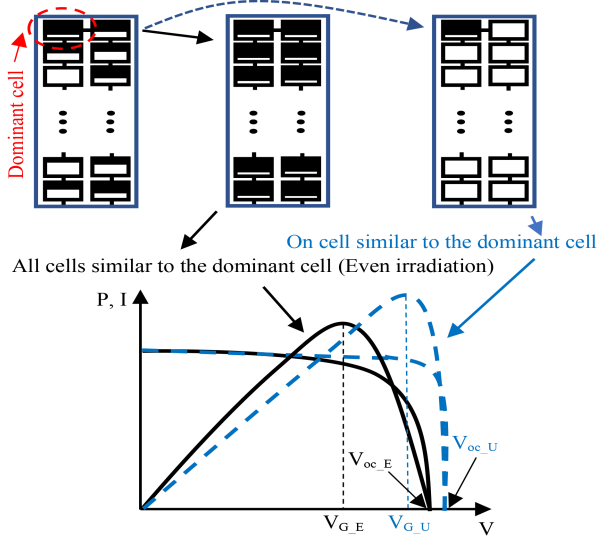
FIGURE 9. *P–V* and current versus voltage for even and uneven irradiation condition (The black solid curve is for the PV panel in which all cells have the shading rate equal to the dominant cell and the blue dashed curve is for the PV panel in which just one cell has the shading rate equal to the dominant cell).

FIGURE 10. *I–V* curves and the GMPPs for ET-M53695 PV panel in different temperatures and shading conditions.
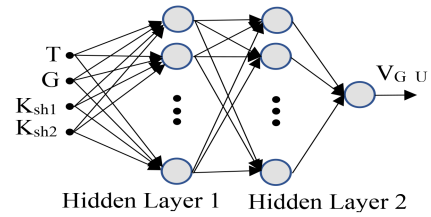
FIGURE 11. Neural network to estimate the GMPP for a panel with two modules.

while V_{G_U} can be determined based on the dominant cell of a PV module using an AI technique. It is worth mentioning that these boundaries can be used as the search space for estimating the proper initial condition for MPPT algorithms.

A. GMPP UNDER EVEN IRRADIATION
Equation (3) shows the current of a module (I) composed of N_g PV cells as a function of its voltage (V) in even irradiation

$$I = I_{ph} - I_o \left(e^{\frac{q(V+R_{SG}I)}{aN_gK_tT}} - 1 \right) - \frac{(V + R_{SG}I)}{R_{PG}}$$

$$R_{SG} = N_gR_S, \quad R_{PG} = N_gR_P \tag{3}$$

where R_{SG} and R_{PG} are series and parallel resistance for a module. The generate power can be expressed as a function of voltage by multiplying both sides of (3) by the voltage. Setting the derivative of power with respect to voltage to zero and applying a Taylor expansion of exponential function results in the voltage value at the GMPP, which can be calculate by (4) and is equal to U_{G_U}

$$V_{G\_U} = V_{GMPP} = \left(V_{oc} + \frac{2}{m} \right) - \sqrt{\frac{2}{m}V_{oc} + \frac{4}{m^2}}$$

$$m = \frac{q}{aN_gK_tT}. \tag{4}$$

B. GMPP UNDER UNEVEN IRRADIATION AND ESTIMATION OF THE CONVEX AREA
An MPPT algorithm guarantees finding the GMPP when the *I–V* curve is convex. But the *I–V* curve of the PV panel in PS condition is not convex; therefore, this algorithm may get stuck in the LMPP. To solve this problem, the convex
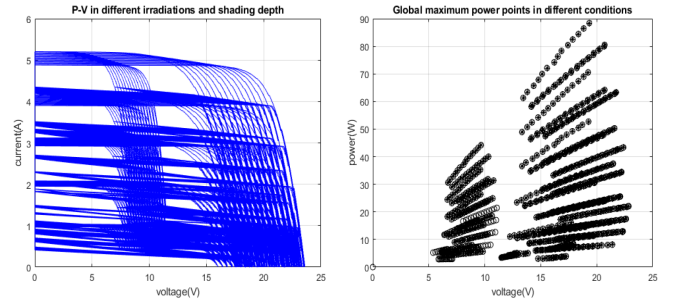
area around the GMPP can be detected as the tracking area. Using this method, not only finding the GMPP is guaranteed, but also the speed of tracking will increase significantly. As explained in the previous sections, GMPP is between V_{G_E} and V_{G_U}; therefore, these values determine the tracking area for the MPPT algorithm. Usually PV panels have 1, 2, or 3 modules depending on the number of PV cells. As a case study, a PV panel with 2 modules and N_g cells in each module is used for simplicity. In this way, the acquired knowledge can be generalized easily to a PV panel with more than 2 modules. Each module in this panel in PS conditions has one dominant cell in shading conditions while the remaining $N_g - 1$ cells have an even irradiation. The *I–V* curve of the dominant cell as well as other cells in the even irradiation can be achieved numerically for each module under non STC using (2). Then, the upper boundary of the *I–V* curve for each module can be determined using the method explained in Fig. 5. Finally, the upper boundary of the *I–V* curve for a panel can be obtained based on the hypothesis highlighted in Fig. 8. Therefore, V_{G_U} for each condition can be calculated. In this way, a series of *I–V* curves related to the dominant cells for the ET-M53695 PV panel under different conditions and their GMPP are shown in Fig. 10. It can be seen that V_{G_U} is a function of temperature, irradiation and coefficients representing the depths of shading (K_{sh1} and K_{sh2} for ET-M53695 PV panel, which has two modules). An AI technique could be a powerful tool train and estimate this function. Fig. 11 shows this network for a panel with two modules. It has as inputs the temperature, irradiation, and coefficients for dominant_cells and as output the voltage at the upper boundary. The chosen neural network architecture has two hidden layers with 5 neurons in each
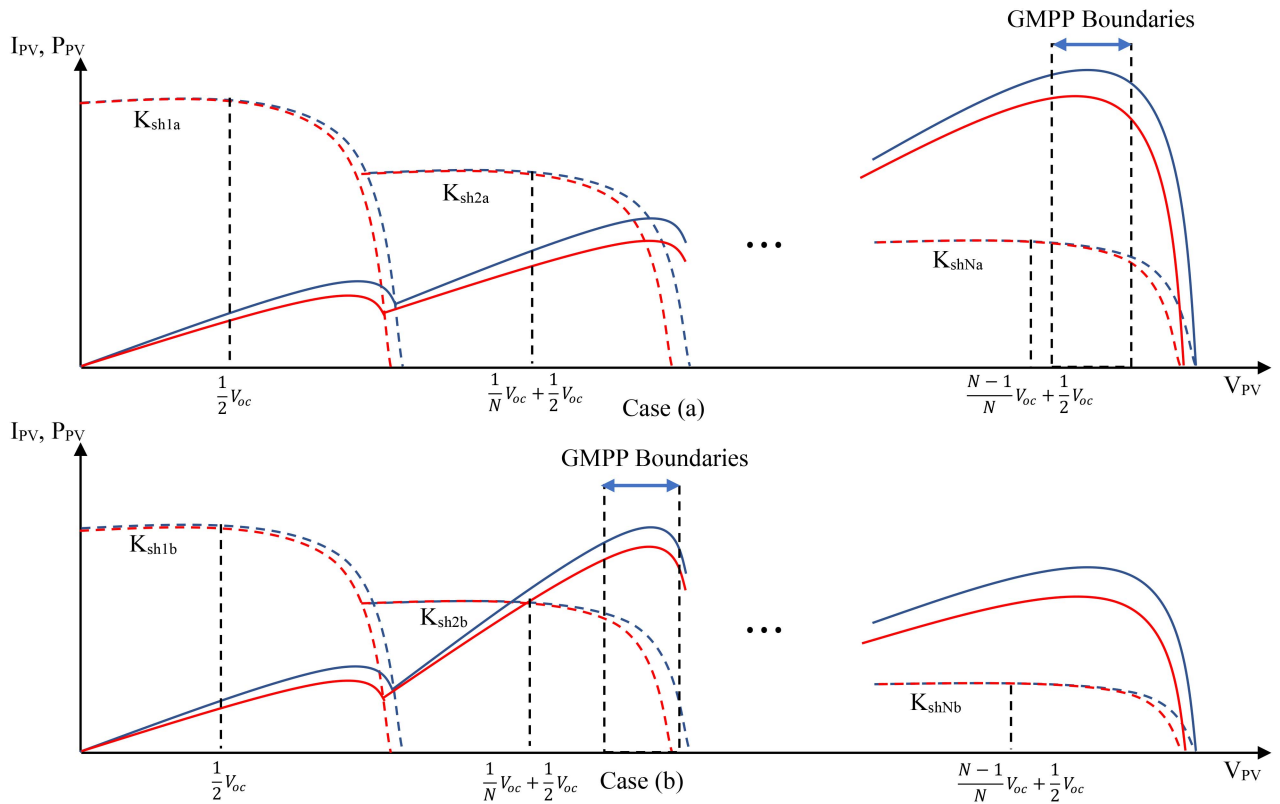
FIGURE 12. GMPP upper and lower boundaries in a system with N PV modules (blue dashed line: the upper *I–V* boundary, red dashed line: the lower *I–V* boundary, blue solid line: the upper *P–V* boundary, and red solid line: the lower *P–V* boundary).

layer (determined experimentally) and one neuron in the output layer. The lower boundary of the GMPP can be calculated using (4). As mentioned, the GMPP will occur somewhere between the lower and the upper boundaries; therefore, the average of these points is the best choice as an initial condition for the MPPT algorithm.

C. GMPP BOUNDARIES ESTIMATOR FOR A GENERAL CASE

Fig. 12 illustrates the proposed initial point estimator for a PV system comprising N PV panels. Case (a) and (b) show two PS conditions when the temperature (T) and irradiation value (G) is the same while each PV panel has different shading rate value (K_{shia} for case (a) and K_{shib} for case (b), $i = 1, 2, \ldots, N$). The upper and lower boundaries are shown for both cases and for all PV modules. As seen, the GMPP voltage value is between two boundaries for each case. In other words, if the temperature, irradiation value, and shading rate for each module are available, theses boundaries for these conditions can be calculated. A dataset is prepared by changing theses values as the input data and the upper boundary or the average of these boundaries as the output. Then, a neural network as depicted in Fig. 13, is trained for this system, which is used as the initial point estimator for the GMPP tracking algorithm. The temperature (T) and irradiation value (G) are measured by their sensors. Also, the shading rate is measured by setting the output voltage of the PV system from
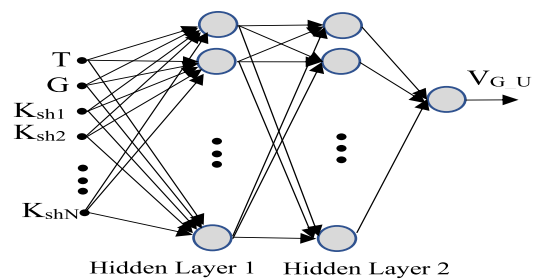

FIGURE 13. Neural network to estimate the GMPP for a system with N PV modules.

$(\frac{N-1}{N} + \frac{1}{2})V_{oc}$, $(\frac{N-2}{N} + \frac{1}{2})V_{oc}, \ldots, \frac{1}{2}V_{oc}$ as seen in Fig. 12 and measuring the short-circuit current of each PV module. As seen from Fig. 5, the shading rate of a PV panel is proportional to the short-circuit current, therefore, these shading rates are measured to estimate the initial point at the beginning of the GMPP tracking algorithm or whenever the PS is detected. Under dynamic conditions, detecting the shading rate of the dominant cells is also performed whenever the irradiation or PS condition pattern changes. In MPPT algorithms, the PS conditions or changes in the irradiation are detected when the difference between two consecutive samples of the generated power is greater than a predefined value. Therefore, when this condition occurs, the system starts the initial point estimation
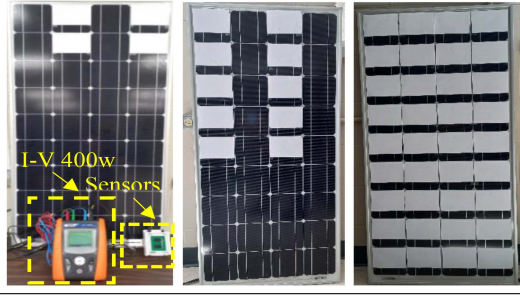
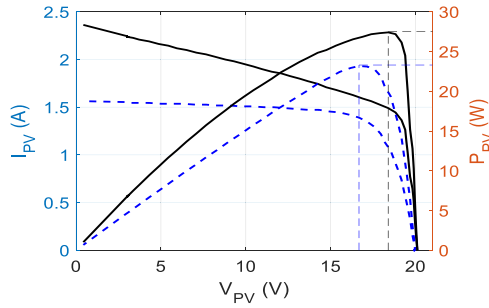**FIGURE 14.** Photos of PV panel with some shading patterns.

FIGURE 15. *I–V* and *P–V* curves for one and all cells in shading condition for ET-M53695 PV panel measured by *I–V* 400 w (Solid curves for one cell (dominant cell) in PS condition and dashed curves for even shading).

FIGURE 16. Prepared PV system to implement the proposed method.

TABLE 1. Parameters of the System

Parameter	Description	Value
V_o	Output voltage	50 V
f_{sw}	Switching frequency	20 kHz
C_{in}	Input capacitor	220 μF
C_o	Output capacitor	220 μF
L	Converter inductor	1 mH

FIGURE 17. *P–V* curve of the PV panel.

by measuring the shading rate of the dominant cells, as explained above.

V. EXPERIMENTAL RESULTS

In order to examine the performance of the proposed GMPP estimator, the ET-M53695 PV panel in different shading conditions is used as shown in Fig. 14. The values for I_{ph}, I_o, R_S, R_P, and a for this panel are 5.0 A, 0.224 μA, 0.226 Ω, 1670 Ω, and 1.398, respectively. These values are calculated by measuring the current and voltage at several operating points and applying the Newton–Raphson method to solve the single diode model of the PV panel in (3). The shading conditions were produced manually and the *I–V* 400w PV Panel Analyzer was used to measure the *I–V* and *P–V* curves. The upper and lower boundary of *I–V* and *P–V* curves of this panel are shown in Fig. 15 when one or all cells are in the shading condition. As seen, the voltage at the GMPP occurs between these two boundaries as it was explained in Figs. 7 and 9. In this case, it was between 16.67 V and 18.39 V. V_{oc} and m were 20.1 V and 1.73, respectively, therefore, the voltage at the GMPP (the lower boundary) can be calculated using (4), which is equal to 16.30 V. Also, the upper boundary can be calculated using the model. The temperature, irradiation, and depth of shading for both modules (K_{sh1} and K_{sh2}) were 32°C, 486 $\frac{W}{m^2}$, and 0.6, respectively. The upper boundary of the model is 18.27 V. In general, the boundaries of the voltage at the GMPP are estimated between 16.30 V and 18.27 V. The prediction error achieved in comparison to their real value
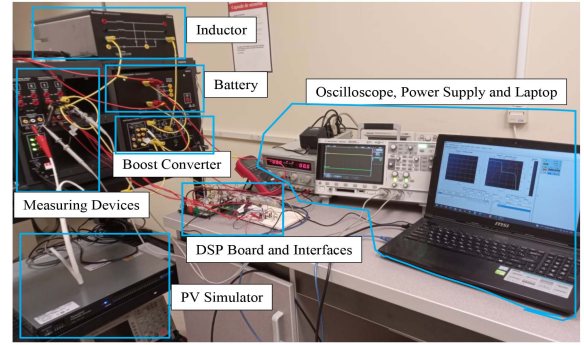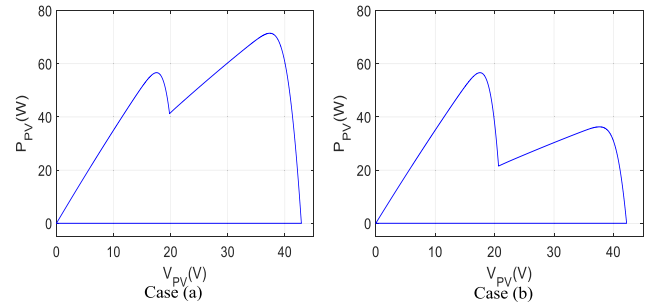
(i.e., 16.67 V and 18.39 V) is low enough (i.e., 2.22% error for lower boundary and 0.65% error for upper boundary).

An experimental setup was prepared to evaluate the performance of the MPPT algorithm using the proposed method, as shown in Fig. 16. This setup mainly consists of a boost power optimizer, battery and some resistors in parallel as a dc load, TerraSAS PV simulator to generate *P–V* curves, current and voltage measuring sensors, inductor, and capacitor. The parameters of the experimental setup are shown in Table 1. The MPPT algorithms were implemented using TMS320F28335 DSP microcontroller. As shown in Fig. 17, two scenarios are taken into account to evaluate the performance of the proposed method in comparison with the traditional HC algorithm. It should be emphasized that almost all traditional MPPT algorithms such as HC or P&O or heuristics and more sophisticated methods such as grey wolf optimization and PSO require initial points. If these initial points estimated correctly, the performance of that method improves significantly. In other words, the result of each MPPT algorithm should be compared with its result when it is equipped with the proposed initial point of this article. In this article, the HC
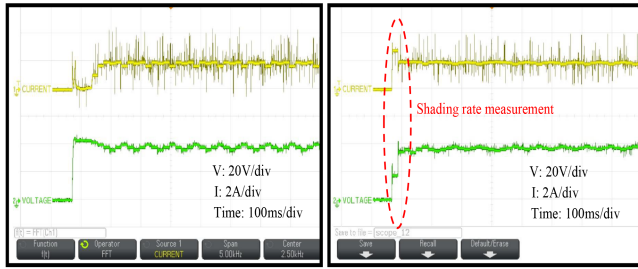
FIGURE 18. PV voltage and current for case (a) (the traditional method on the left and the proposed one on the right).
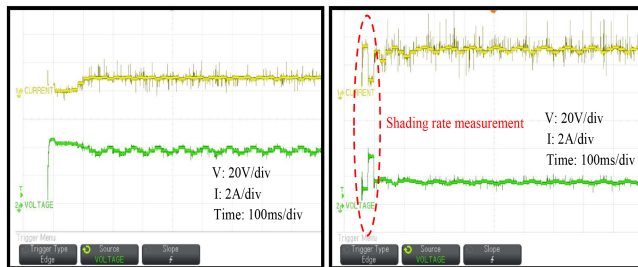

FIGURE 19. PV voltage and current for case (b) (the traditional method on the left and the proposed one on the right).

FIGURE 20. Generated power for case (a) (the traditional method on the left and the proposed one on the right).

FIGURE 21. Generated power for case (b) (the traditional method on the left and the proposed one on the right).

MPPT algorithm is considered to prove the effectiveness of the proposed initial point estimator in the GMPP tracking performance improvement. Fig. 18 shows the current and voltage for the traditional and proposed method for case (a).

As explained in Section IV, the shading rate of each PV panel should be measured at the beginning of the MPPT algorithm or whenever the PS occurs as the input values for the neural network shown in Figs. 11 and 13. This step is shown by a dashed area in the experimental results. After this step, these values and the irradiation and temperature ones build the input data for the neural network model, which provides the initial point for the MPPT algorithm. As can be seen, the proposed MPTT method has a lower convergence time to find the GMPP (250 ms for the traditional HC in comparison to 100 ms for the proposed method). Moreover, the fluctuations in the steady state improved using the proposed method.

Fig. 19 shows the current and voltage for the traditional and proposed method for case (b). As expected, the traditional HC algorithm gets stuck in the local MPP (37.5 V) while for the proposed MPPT algorithm the GMPP (17.5 V in this case) is guaranteed due to the accurate detection of the GMPP boundaries using the proposed estimator.

Figs. 20 and 21 show the generated power for both algorithms under cases (a) and (b). As seen, in comparison with the traditional method, the power fluctuations using the proposed method over the period of finding the GMPP as well as in the steady state are considerably improved. In addition, Fig. 21 shows that the PV system generates a lower power using the traditional method (37 W) rather than the proposed MPPT technique (57 W), highlighting the fact that the traditional HC MPPT is unable to find the GMPP.
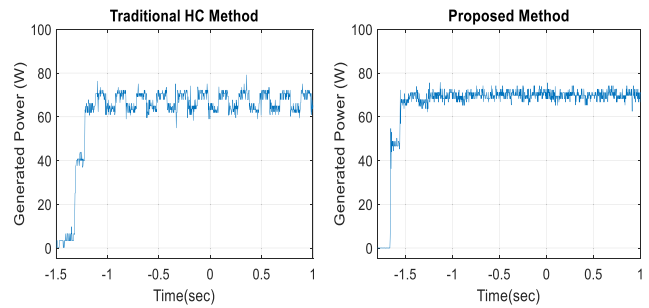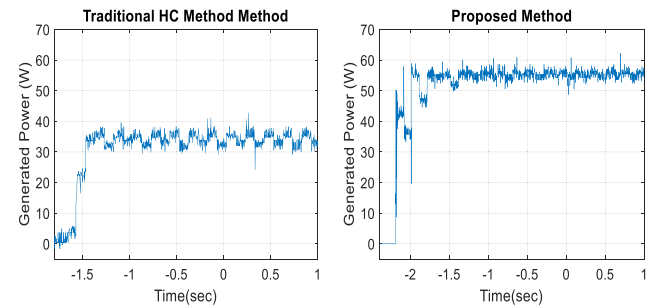
VI. CONCLUSION

In this article, a GMPP estimator was proposed as a global solution for MPPT algorithms under PS conditions. To this end and for an effective analysis of the PS condition, the concept of a dominant cell in a module of a PV panel is proposed that can reduce the infinite number of potential PS patterns. Then, the lower and upper voltage boundaries to track the GMPP with a rapid convergence and small fluctuations were proposed. The lower voltage boundary was determined using a closed-form formula, while the upper one was determined using an AI technique. In addition, these boundaries were used to determine an initial condition for MPPT algorithms. The proposed GMPP estimator was then applied to a traditional HC MPPT algorithm. An experimental setup was built to evaluate the capability of the proposed technique. The experimental results under different PS conditions validated the proposed technique effectiveness since the GMPP was successfully tracked with a low convergence time and small fluctuations.

REFERENCES

[1] V. K. Kolakaluri, M. N. Aalam, and V. Sarkar, "Metaheuristics assisted efficiency maximizing flexible power point tracking of a photovoltaic array under the partial shading," *IEEE Trans. Energy Convers.*, vol. 38, no. 3, pp. 1576–1588, Sep. 2023.

[2] V. M. R. Tatabhatia, A. Agarwal, and T. Kanumuri, "A chaos map based reconfiguration of solar array to mitigate the effects of partial shading," *IEEE Trans. Energy Convers.*, vol. 37, no. 2, pp. 811–823, Jun. 2022.

[3] R. Sangrody, S. Taheri, and E. Pouresmaeil, "High-efficient photovoltaic power optimizer based on the intrinsic resonance and coupled inductors," *IEEE Trans. Ind. Electron.*, vol. 72, no. 8, pp. 8049–8059, Aug. 2025.

[4] A. Ostadrahimi and Y. Mahmoud, "Novel Spline-MPPT technique for photovoltaic systems under uniform irradiance and partial shading conditions," *IEEE Trans. Sustain. Energy*, vol. 12, no. 1, pp. 544–532, Jan. 2021.

[5] Y. Mahmoud and E. F. El-Saadany, "Enhanced reconfiguration method for reducing mismatch losses in PV systems," *IEEE J. Photovolt.*, vol. 7, no. 6, pp. 1746–1754, Nov. 2017.

[6] S. R. Pendem, S. Mikkili, and P. K. Bonthagorla, "PV Distributed-MPP tracking: Total-cross-tied configuration of string-integrated-converters to extract the maximum power under various PSCs," *IEEE Syst. J.*, vol. 14, no. 1, pp. 1046–1057, Mar. 2020.

[7] B. K. Karmakar and G. Karmakar, "A current supported PV array reconfiguration technique to mitigate partial shading," *IEEE Trans. Sustain. Energy*, vol. 12, no. 2, pp. 1449–1460, Apr. 2021.

[8] J. C. Teo, R. H. G. Tan, V. H. Mok, V. K. Ramachandaramurthy, and C. Tan, "Impact of partial shading on the P-V characteristics and the maximum power of a photovoltaic string," *Energies*, vol. 11, no. 7, Jul. 2018, Art. no. 1860.

[9] W. Zhu, L. Shang, P. Li, and H. Guo, "Modified Hill climbing MPPT algorithm with reduced steady-state oscillation and improved tracking efficiency," *J. Eng.*, vol. 2018, no. 17, pp. 1878–1883, Nov. 2018.

[10] M. Joisher, D. Singh, S. Taheri, D. R. Espinoza-Trejo, E. Pouresmaeil, and H. Taheri, "A hybrid evolutionary-based MPPT for photovoltaic systems under partial shading conditions," *IEEE Access*, vol. 8, pp. 38481–38492, 2020.

[11] S. Mohanty, B. Subudhi, and P. K. Ray, "A grey wolf-assisted perturb & observe MPPT algorithm for a PV system," *IEEE Trans. Energy Convers.*, vol. 32, no. 1, pp. 340–347, Mar. 2017.

[12] C. Pradhan, M. K. Senapati, S. G. Malla, P. K. Nayak, and T. Gjengedal, "Coordinated power management and control of standalone PV-Hybrid system with modified IWO-Based MPPT," *IEEE Syst. J.*, vol. 15, no. 3, pp. 3585–3596, Sep. 2021.

[13] P. Manoharan et al., "Improved perturb and observation maximum power point tracking technique for solar photovoltaic power generation systems," *IEEE Syst. J.*, vol. 15, no. 2, pp. 3024–3035, Jun. 2021.

[14] J. P. Ram, D. S. Pillai, N. Rajasekar, and S. M. Strachan, "Detection and identification of global maximum power point operation in solar PV applications using a hybrid ELPSO-P&O tracking technique," *IEEE Trans. Emerg. Sel. Topics Power Electron.*, vol. 8, no. 2, pp. 1361–1374, Jun. 2020.

[15] I. Shams, S. Mekhilef, and K. S. Tey, "Improved-team-Game-Optimization-Algorithm-Based solar MPPT with fast convergence speed and fast response to load variations," *IEEE Trans. Ind. Electron.*, vol. 68, no. 8, pp. 7093–7103, Aug. 2021.

[16] Y. P. Huang, M. Y. Huang, and C. E. Ye, "A fusion firefly algorithm with simplified propagation for photovoltaic MPPT under partial shading conditions," *IEEE Trans. Sustain. Energy*, vol. 11, no. 4, pp. 2641–2652, Oct. 2020.

[17] K. Guo, L. Cui, M. Mao, L. Zhou, and Q. Zhang, "An improved gray wolf optimizer MPPT algorithm for PV system with BFBIC converter under partial shading," *IEEE Access*, vol. 8, pp. 103476–103490, 2020.

[18] R. Sangrody, S. Taheri, A. M. Cretu, and E. Pouresmaeil, "An improved PSO-based MPPT technique using stability and steady state analyses under partial shading conditions," *IEEE Trans. Sustain. Energy*, vol. 15, no. 1, pp. 136–145, Jan. 2024.

[19] S. G. Malla et al., "Whale optimization algorithm for PV based water pumping system driven by BLDC motor using sliding mode controller," *IEEE Trans. Emerg. Sel. Topics Power Electron.*, vol. 10, no. 4, pp. 4832–4844, Aug. 2022.

[20] S. Lyden, H. Galligan, and M. E. Haque, "A hybrid simulated annealing and perturb and observe maximum power point tracking method," *IEEE Syst. J.*, vol. 15, no. 3, pp. 4325–4333, Sep. 2021.

[21] C. Gonzalez-Castano, C. Restrepo, S. Kouro, and J. Rodriguez, "MPPT algorithm based on artificial bee colony for PV system," *IEEE Access*, vol. 9, pp. 43121–43133, 2021.

[22] K. Xia, Y. Li, and B. Zhu, "Improved photovoltaic MPPT algorithm based on ant colony optimization and fuzzy logic under conditions of partial shading," *IEEE Access*, vol. 12, pp. 44817–44825, 2024.

[23] D. A. Nugraha, K. L. Lian, and Suwarno, "A novel MPPT method based on cuckoo search algorithm and golden section search algorithm for partially shaded PV system," *Can. J. Elect. Comput. Eng.*, vol. 42, no. 3, pp. 173–182, Jul. 2019.

[24] R. R. P, V. K. V, K. K. Prabhakaran, and B. Venkatesaperumal, "A novel algorithm based on voltage and current perturbation to track global peak under partial shading conditions," *IEEE Trans. Energy Convers.*, vol. 37, no. 4, pp. 2461–2471, Dec. 2022.

[25] S. Hosseini, S. Taheri, M. Farzaneh, and H. Taheri, "A high-performance shade-tolerant MPPT based on current-mode control," *IEEE Trans. Power Electron.*, vol. 34, no. 10, pp. 10327–10340, Oct. 2019.

[26] S. Selvakumar, M. Madhusmita, C. Koodalsamy, S. P. Simon, and Y. R. Sood, "High-speed maximum power point tracking module for PV systems," *IEEE Trans. Ind. Electron.*, vol. 66, no. 2, pp. 1119–1129, Feb. 2019.

[27] R. Sangrody and S. Taheri, "An online scanning method to detect the output characteristics of photovoltaic panels," *IEEE Trans. Ind. Electron.*, vol. 71, no. 9, pp. 10831–10840, Sep. 2024.

[28] A. M. S. Furtado, F. Bradaschia, M. C. Cavalcanti, and L. R. Limongi, "A reduced voltage range global maximum power point tracking algorithm for photovoltaic systems under partial shading conditions," *IEEE Trans. Ind. Electron.*, vol. 65, no. 4, pp. 3252–3262, Apr. 2018.

[29] S. Madichetty, S. Mishra, and A. J. Neroth, "Maximum power point in a single step: A novel method for PV industry," *IEEE Power Electron. Mag.*, vol. 8, no. 3, pp. 48–54, Sep. 2021.

[30] X. Meng, F. Gao, T. Xu, and C. Zhang, "Fast two-stage global maximum power point tracking for grid-tied string PV inverter using characteristics mapping principle," *IEEE Trans. Emerg. Sel. Topics Power Electron.*, vol. 10, no. 1, pp. 564–574, Feb. 2022.

[31] H. M. El-Helw, A. Magdy, and M. I. Marei, "A hybrid maximum power point tracking technique for partially shaded photovoltaic arrays," *IEEE Access*, vol. 5, pp. 11900–11908, 2017.

[32] W. Zhang, G. Zhou, H. Ni, and Y. Sun, "A modified hybrid maximum power point tracking method for photovoltaic arrays under partially shading condition," *IEEE Access*, vol. 7, pp. 160091–160100, 2019.

[33] S. Allahabadi, H. Iman-Eini, and S. Farhangi, "Fast artificial neural network based method for estimation of the global maximum power point in photovoltaic systems," *IEEE Trans. Ind. Electron.*, vol. 69, no. 6, pp. 5879–5888, Jun. 2022.

[34] A. G. Galeano, M. Bressan, F. J. Vargas, and C. Alonso, "Shading ratio impact on photovoltaic modules and correlation with shading patterns," *Energies*, vol. 11, no. 4, Apr. 2018, Art. no. 852.

[35] Y. Mahmoud and E. F. El-Saadany, "A novel MPPT technique based on an image of PV modules," *IEEE Trans. Energy Convers.*, vol. 32, no. 1, pp. 213–221, Mar. 2017.

[36] M. K. Al-Smadi and Y. Mahmoud, "Image-based differential power processing for photovoltaic microinverter," *IEEE Trans. Energy Convers.*, vol. 36, no. 2, pp. 619–628, Jun. 2021.

[37] M. Dhimish, V. Holmes, B. Mehrdadi, M. Dales, and P. Mather, "Output-power enhancement for hot spotted polycrystalline photovoltaic solar cells," *IEEE Trans. Device Mater. Rel.*, vol. 18, no. 1, pp. 37–45, Mar. 2018.

[38] Y. Hu, W. Cao, J. Wu, B. Ji, and D. Holliday, "Thermography-based virtual MPPT scheme for improving PV energy efficiency under partial shading conditions," *IEEE Trans. Power Electron.*, vol. 29, no. 11, pp. 5667–5672, Nov. 2014.

REZA SANGRODY received the Ph.D. degree in information science and technology from Université du Québec en Outaouais (UQO), Gatineau, QC, Canada, in 2025.

Following his Ph.D., he began working in the Canadian high-technology industry, focusing on electronics and power electronic applications. His current research interests include power electronic circuit design and control, applications of power electronic converters in smart grids, photovoltaic and wind energy generation, and electric machine drive systems.

SHAMSODIN TAHERI (Senior Member, IEEE) received the B.Sc. degree from the University of Mazandaran, Babolsar, Iran, in 2006, the master's degree from the Iran University of Science and Technology (IUST), Tehran, Iran, in 2009, and the Ph.D. degree from the University of Quebec in Chicoutimi (UQAC), Chicoutimi, QC, Canada, in 2013, all in electrical engineering.

From 2013 to 2014, he worked with Technical Services and Research Department, Saskpower, Regina, SK, Canada. Since 2014, he has been a Professor with the University of Quebec in Outaouais, Gatineau, QC. His research focuses on integrating renewable energy sources into power grids under cold climate conditions, with expertise in photovoltaic systems. He is the founder of LAR3E, a CFI-funded laboratory on energy efficiency in power networks.

ANA-MARIA CRETU (Senior Member, IEEE) received the Ph.D. degree in electrical and computer engineering from the School of Electrical Engineering and Computer Science, University of Ottawa, Ottawa, ON, Canada, in 2009.

She is currently a Professor with the Department of Computer Science and Engineering, Université du Québec en Outaouais, Gatineau, QC, Canada. Her research interests include computational intelligence, soft computing, biologically inspired computational models, tactile and vision sensing, and 3-D object sensing, modeling and manipulation.

Dr. Cretu is currently a Reviewer for journals and transactions and as an Associate Editor for *Springer Soft Computing Journal*. She is a Member of the Ordre des Ingénieurs du Québec.

EDRIS POURESMAEIL (Senior Member, IEEE) received the Ph.D. degree in electrical engineering from the Technical University of Catalonia (UPC-Barcelona Tech), Barcelona, Spain, in 2012.

He joined the University of Waterloo, Waterloo, ON, Canada, as a Postdoctoral Research Fellow, and later the University of Southern Denmark, Odense, Denmark, as an Associate Professor. He is currently an Associate Professor with the Department of Electrical Engineering and Automation, Aalto University, Espoo, Finland. His research focuses on power electronics for power systems, the integration of renewable energy sources into power grids, microgrid control and operation, and hybrid energy storage systems using green hydrogen and batteries.

Dr. Pouresmaeil is currently an Associate Editor for IEEE TRANSACTIONS ON SMART GRID, IEEE SYSTEM JOURNAL, IEEE OPEN JOURNAL OF THE INDUSTRIAL ELECTRONICS SOCIETY, IEEE OPEN JOURNAL OF POWER ELECTRONICS, and *IET Generation, Transmission and Distribution*.

HANI VAHEDI (Senior Member, IEEE) received the Ph.D. (Hons.) degree in electrical engineering from École de Technologie Superieure (ÉTS), University of Quebec, Montreal, QC, Canada, in 2016.

After 7 years of experience in industry as a Power Electronics Designer and Chief Scientific Officer, he joined the Delft University of Technology (TU Delft), Delft, The Netherlands, where he is currently an Assistant Professor with the DCE&S group, working toward the electrification of industrial processes for clean energy transition. He is also leading the 24/7 Energy Hub project at The Green Village of TU Delft, implementing a local microgrid with renewable energy resources, green Hydrogen production, and energy storage systems as the future of the clean energy transition. He has authored or coauthored more than 100 technical papers in IEEE conferences and transactions. He also authored or coauthored a book on Springer Nature and a book chapter in Elsevier. His research interests include multilevel converter topologies, control and modulation techniques, and their applications in the electrification of industrial processes and clean energy transition, such as smart grids, renewable energy conversion, electric vehicle chargers, green hydrogen production (electrolyzers), and fuel-cell systems.

Dr. Vahedi was a Co-Chair of the IEEE Industrial Electronics Society (IES) Student and Young Professionals (S&YP) committee and is currently serving as the IES Chapters Coordinator. He has been co-organizing special sessions and SYP forums at IEEE international conferences. He is also the Associate Editor for IEEE TRANSACTIONS ON INDUSTRIAL ELECTRONICS, *Open Journal of Industrial Electronics*, and *Open Journal of Power Electronics*. He is the inventor of the PUC5 converter, holds multiple U.S./world patents, and transferred that technology to the industry, where he developed the first bidirectional electric vehicle dc charger based on his invention. He was the recipient of the Best Ph.D. Thesis Award from ETS for the academic year of 2016–2017.